Boronic acid-based inhibitor of autotaxin reveals rapid turnover of LPA in the circulation

Harald M. H. G. Albers[a,b], Anping Dong[c], Laurens A. van Meeteren[a], David A. Egan[d], Manjula Sunkara[c], Erica W. van Tilburg[a], Karianne Schuurman[a], Olaf van Tellingen[e], Andrew J. Morris[c], Susan S. Smyth[c], Wouter H. Moolenaar[a,f], and Huib Ovaa[a,b,1]

[a]Division of Cell Biology, [b]Netherlands Proteomics Centre, [f]Centre of Biomedical Genetics, [d]Division of Molecular Carcinogenesis, and [e]Department of Clinical Chemistry, The Netherlands Cancer Institute, 1066 CX Amsterdam, The Netherlands; and [c]Division of Cardiovascular Medicine, University of Kentucky, Lexington, KY 40536

Communicated by Joseph Schlessinger, Yale University School of Medicine, New Haven, CT, February 16, 2010 (received for review October 21, 2009)

Autotaxin (ATX) is a secreted nucleotide pyrophosphatase/phosphodiesterase that functions as a lysophospholipase D to produce the lipid mediator lysophosphatidic acid (LPA), a mitogen, chemoattractant, and survival factor for many cell types. The ATX-LPA signaling axis has been implicated in angiogenesis, chronic inflammation, fibrotic diseases and tumor progression, making this system an attractive target for therapy. However, potent and selective nonlipid inhibitors of ATX are currently not available. By screening a chemical library, we have identified thiazolidinediones that selectively inhibit ATX-mediated LPA production both in vitro and in vivo. Inhibitor potency was approximately 100-fold increased ($IC_{50} \sim 30$ nM) after the incorporation of a boronic acid moiety, designed to target the active-site threonine (T210) in ATX. Intravenous injection of this inhibitor into mice resulted in a surprisingly rapid decrease in plasma LPA levels, indicating that turnover of LPA in the circulation is much more dynamic than previously appreciated. Thus, boronic acid-based small molecules hold promise as candidate drugs to target ATX.

high-throughput screening | lysophosphatidic acid | lysophospholipase D | small-molecule inhibitor | phosphodiesterase

Autotaxin (ATX or NPP2) is a secreted nucleotide pyrophosphatase/phosphodiesterase (NPP) originally isolated as an autocrine motility factor from melanoma cells (1). ATX, a ~120 kDa glycoprotein, is unique amongst the NPPs in that it functions as a lysophospholipase D (lysoPLD) that converts extracellular lysophosphatidylcholine (LPC) into the lipid mediator lysophosphatidic acid (LPA; mono-acyl-*sn*-glycero-3-phosphate) (2–5). LPA acts on specific G protein-coupled receptors and thereby stimulates the migration, proliferation, and survival of many cell types (6 and 7) (Fig. 1). ATX is produced by various tissues and is the major LPA-producing enzyme in the circulation. Newly produced LPA is subject to degradation by membrane-bound lipid phosphate phosphatases (LPPs) (8 and 9). However, little is known about the dynamic regulation of steady-state LPA levels in vivo.

ATX is essential for vascular development (10 and 11) and is found overexpressed in various human cancers (12). Forced overexpression of ATX or individual LPA receptors promotes tumor progression in mouse models (13–16), while LPA receptor deficiency protects from colon carcinogenesis (17). In addition to its role in cancer, ATX-LPA signaling has been implicated in lymphocyte homing and (chronic) inflammation (18), fibrotic diseases (19 and 20), and thrombosis (21). Therefore, the ATX-LPA axis qualifies as an attractive target for therapies.

Potent and selective ATX inhibitors are now needed as a starting point for the development of targeted anti-ATX/LPA therapy. Direct targeting of LPA receptors seems to be a less attractive strategy, since LPA acts on multiple receptors that show overlapping activities (2 and 6). Since the initial finding that ATX is subject to product inhibition by LPA and sphingosine 1-phosphate (S1P) (22), various synthetic phospho- and phosphonate lipids have been explored as ATX inhibitors (23–26). However, such lipid inhibitors have the inherent danger of inadvertently activating downstream LPA/S1P receptors, thereby inducing the opposite of the intended effect. Furthermore, lipids offer relatively few avenues for chemical diversification and usually have poor pharmacokinetic properties. Nonlipid inhibitors of ATX have recently been identified, but their potencies are low (27).

In this study we screened small-molecule libraries to search for unique ATX inhibitors. We identified thiazolidinedione compounds that selectively inhibit ATX activity and are readily amenable to further chemical diversification. We have optimized these molecules by adopting an active-site-targeted strategy that has proved successful for the development of the boronic acid-based proteasome inhibitor bortezomib (28), which is in clinical use (29). We show that a boronic acid-based inhibitor potently inhibits ATX both in vitro and in vivo. When administered to mice, our compound (**HA130**) induces a remarkably rapid fall in plasma LPA levels, indicating that the turnover of circulating LPA is much more dynamic than previously appreciated. We conclude that boronic acid-based inhibitors hold promise as candidate drugs to target the ATX-LPA axis in vivo.

Results

Discovery of Small-Molecule Inhibitors of ATX. The hydrolytic activity of ATX originates from a single catalytic site at threonine 210 (T210) in the central phosphodiester domain (5) (Fig. 1). To discover unique ATX inhibitors, we screened a collection of ~40,000 drug-like small molecules using the hydrolysis of bis(4-nitrophenyl) phosphate (bis-pNPP) by ATX as a readout. Among the most potent hits, we selected a thiazolidinedione series for optimization since the thiazolidinedione core is readily amenable to chemical diversification (Fig. 2*A*). Inhibitor (**A**) showed an IC_{50} value of 56 nM using 1 mM bis-pNPP as substrate. For validation of **A**, we measured the inhibition of the ATX-catalyzed release of choline from LPC. We established that recombinant ATX has a K_m value for LPC of 94 μM (Fig. S1). Compound **A** inhibited ATX with an IC_{50} value of 2.5 μM using 40 μM LPC as a substrate (Fig. 3*A*). However, it should be noted that **A** has a 35% residual ATX activity (Fig. 3*B*). Inhibition of ATX-mediated LPA production was confirmed by measuring

Author contributions: H.M.H.G.A., L.A.v.M., D.A.E., O.v.T., A.J.M., S.S.S., W.H.M., and H.O. designed research; H.M.H.G.A., A.D., L.A.v.M., D.A.E., M.S., E.W.v.T., K.S., O.v.T., and H.O. performed research; H.M.H.G.A., L.A.v.M., D.A.E., E.W.v.T., A.J.M., S.S.S., and H.O. contributed new reagents/analytic tools; H.M.H.G.A., A.D., L.A.v.M., D.A.E., M.S., E.W.v.T., K.S., O.v.T., A.J.M., S.S.S., W.H.M., and H.O. analyzed data; and H.M.H.G.A., W.H.M., and H.O. wrote the paper.

The authors declare no conflict of interest.

Freely available online through the PNAS open access option.

[1]To whom correspondence should be addressed. E-mail: h.ovaa@nki.nl.

This article contains supporting information online at www.pnas.org/cgi/content/full/1001529107/DCSupplemental.

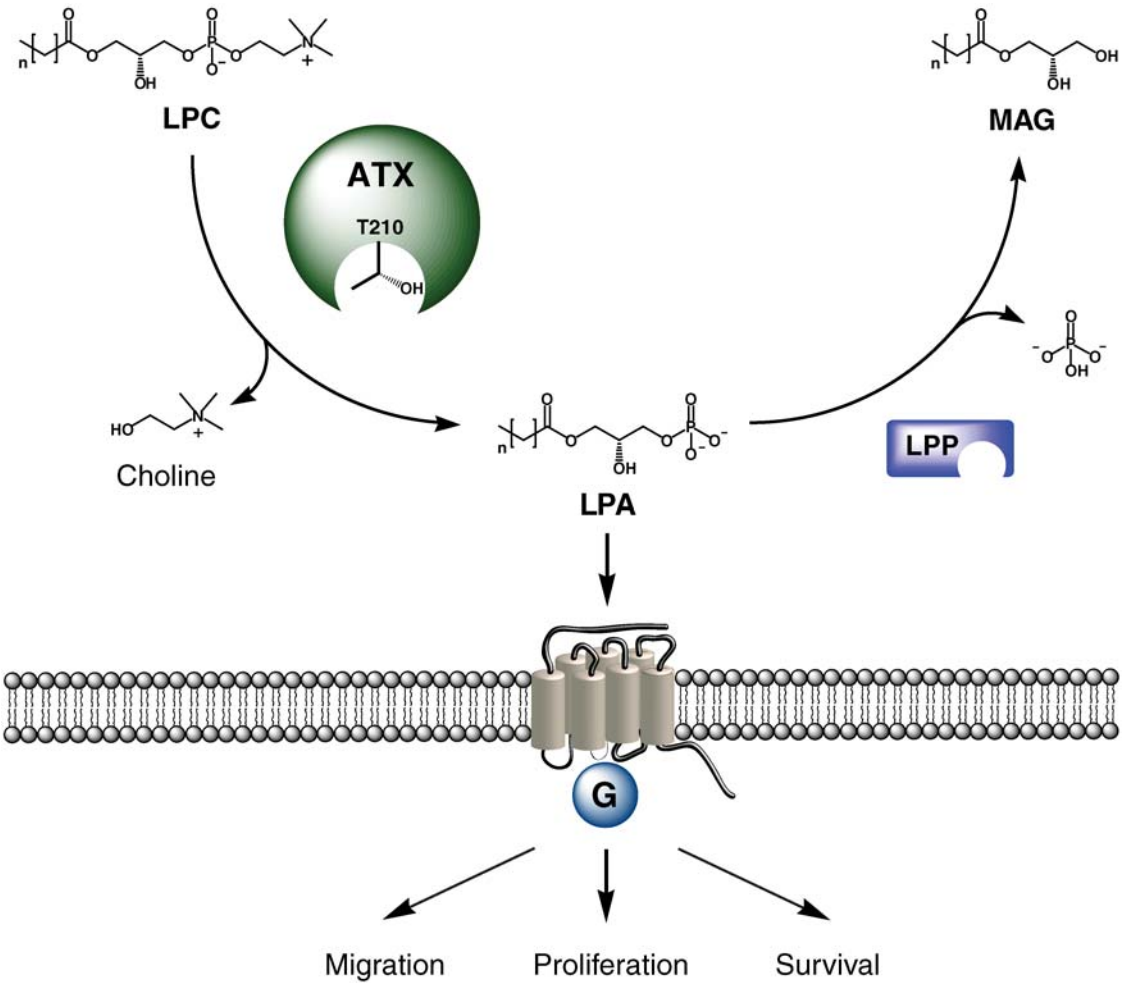

Fig. 1. The ATX-LPA receptor signaling axis. Secreted ATX hydrolyzes extracellular LPC into LPA, a reaction catalyzed by active-site residue T210. LPA signals through multiple G protein-coupled receptors to stimulate the proliferation, migration, and survival of many cell types. LPA is degraded to monoacylglycerol (MAG) by lipid phosphate phosphatases (LPPs), which are membrane-bound ecto-enzymes.

the conversion of ^{14}C-LPC to ^{14}C-LPA using thin-layer chromatography (Fig. 2*B*).

Boronic Acid-Based Optimization. Having identified compound **A** as a unique ATX inhibitor, we set out to improve its potency. Synthesis of **A** required the aldehyde building block **1** (Fig. S2). For this purpose, vanillin was *O*-alkylated with methyl-4-(bromomethyl) benzoate, using potassium hydroxide as a base, to afford the desired methyl benzoate. Benzoic acid **1** was obtained after hydrolysis of methyl benzoate. 2,4-Thiazolidinedione was *N*-alkylated with 4-fluorobenzyl bromide to yield monosubstituted thiazolane-2,4-dione **2**. Knoevenagel condensation of **2** with benzoic acid **1** yielded Z-isomer **A** (Fig. S3). This synthetic route allowed the synthesis and isolation of more than 100 derivatives of **A** in a short time frame.

All derivatives were tested in the ATX-mediated choline release assay. Fig. 3*A* shows the IC_{50} values of the three most important molecules in the optimization process. Omitting the methoxy group and replacing the carboxylic acid to the meta position (**HA51**) resulted in a 2.5-fold increase in potency, concomitant with a significant drop in residual ATX activity, from 35% to 7% (Fig. 3*A*, *B*). Lineweaver-Burk analysis revealed that **A** and **HA51** act as competitive inhibitors (Fig. 3*D*), suggesting that they bind at or close to the catalytic threonine residue (T210).

We next sought to target active-site residue T210. We reasoned that the acid moiety of **A** and **HA51** may strongly bind to the phosphate ester acceptor site in ATX and that the T210 oxygen nucleophile could be targeted by a boronic acid moiety. Boronic acid is known for its high affinity for hard oxygen nucleophiles over soft nucleophiles, such as sulfur which is found in many phosphate ester hydrolytic enzymes. This approach has an important precedent in the proteasome inhibitor and anticancer drug bortezomib (Velcade), which is a peptidyl boronic acid that targets the threonine oxygen nucleophile in the proteasome active site through its boronic acid moiety (28 and 30). We adopted a similar approach to target the T210 oxygen nucleophile in ATX.

Replacing the carboxylic acid in **HA51** by a boronic acid yielded compound **HA130**, that resulted in a ~100-fold increase in potency compared to screening hit **A** (IC_{50} = 28 nM) (Fig. 3*A*). Furthermore, **HA130** abolished the residual ATX activity observed with compounds **A** and **HA51**. Kinetic analysis revealed that **HA130** is a mixed-type inhibitor, producing a reduction in V_{max} and an increase in K_m (Fig. 3*D*). Thus, inhibition of ATX by **HA130** results from a combination of a decreased turnover number and decreased affinity for its substrate. Washout of **HA130** and the other compounds fully restored ATX activity, indicative of reversible inhibition (Fig. 3*C*).

Selective Inhibition of ATX. Since boronic acids can target the proteasome active site, we examined whether **HA130** may affect proteasome activity. **HA130** did not affect the chymotryptic, caspase, and tryptic activities of the proteasome (Fig. S4*B*). Conversely, bortezomib did not affect ATX activity. We next tested

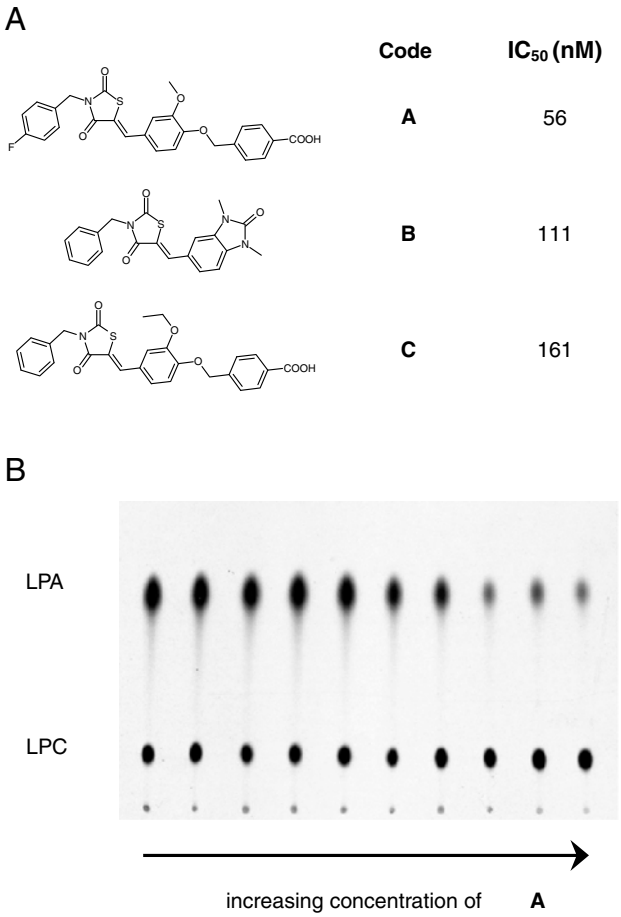

Fig. 2. ATX inhibitors discovered by high-throughput screening and validation of compound **A**. (*A*) IC_{50} values based on bis-pNPP (1 mM) hydrolysis. (*B*) TLC analysis of ^{14}C-LPC to ^{14}C-LPA conversion at different concentrations of **A** (range: 0–30 μM). For details *SI Text*.

our inhibitors for selectivity against recombinant NPP1, which is the closest relative of ATX, alkaline phosphatase (AP) and a broad-spectrum phosphodiesterase (PDE). None of these enzymes were affected by the ATX inhibitors at doses up to 10 μM (Fig. S4*A*). Furthermore, cell viability was not compromised by **HA130** (Fig. S4*C*).

Inhibition of ATX-Driven Melanoma Cell Migration. ATX was originally identified as an autocrine motility factor for human A2058 melanoma cells (1). We examined the ATX-mediated chemotactic migration of A2058 cells using Boyden chamber assays. ATX hydrolyzes exogenously added LPC into LPA, a potent chemoattractant for A2058 cells. As shown in Fig. 4*A*, ATX inhibitors **A**, **HA51**, and **HA130** inhibited ATX-mediated cell migration with increasing potencies. None of the inhibitors affected LPA-induced cell migration, indicating that they do not act on LPA receptor signaling pathways.

Inhibition of Plasma ATX Activity. ATX is identical to plasma lysoPLD (3 and 4) and responsible for virtually all LPA-producing activity in plasma and serum (31). Inhibitors were tested for their ability to inhibit ATX/lysoPLD activity in human plasma ex vivo. As shown in Fig. 4*B*, all three inhibitors were found to inhibit plasma ATX activity with the expected ranking order of potency. Inhibition of plasma ATX activity was long lasting (24 h), indicating that **HA130** is metabolically stable in plasma (Table S1).

HA130 Decreases Circulating LPA Levels in Mice. To investigate how ATX inhibition affects circulating plasma LPA levels, we administered **HA130** (1 nmol g^{-1}) or vehicle as a single bolus injection into the jugular vein of anaesthetized mice. As a nonvehicle control we used compound **HA51**. Levels of **HA130** or LPA in plasma samples rapidly isolated from venous blood were monitored before and after dosing. As shown in Fig. 5*A*, intravenous administration of vehicle or **HA51** (Fig. S5) had little or no effect on plasma LPA levels. Following administration of **HA130** (t = 10 min), plasma levels of the inhibitor rose rapidly to a concentration approaching 0.35 μM. This was accompanied by a parallel decrease in plasma LPA levels (3.8-fold) which returned slowly towards baseline as plasma levels of **HA130** declined. Fig. 5*B* shows summarized data from replicate experiments in which mice were dosed with vehicle or **HA130** while plasma LPA levels were measured before, 2 and 10 min post dosing (see also Fig. S5). Administration of **HA130** produced statistically significant decreases in plasma LPA levels compared to baseline, vehicle, and **HA51**. The mean decrease in plasma LPA levels was 48% of the baseline control at 2 min post administration of **HA130**. Plasma **HA130** levels correlated well ($R^2 = 0.751$) with plasma LPA levels (Fig. 5*C*). Taken together, these findings suggest that continual production of LPA by ATX-catalyzed hydrolysis of circulating LPC is required to sustain plasma levels of LPA at their observed steady-state level. To confirm this, we injected C17-LPA and found that the levels of this unnatural LPA analog were elevated at the earliest measurable time point, but then decayed rapidly following pseudo first-order kinetics with a half-life of approximately 3 min. (Fig. 5*D*).

Discussion

ATX is a secreted lysoPLD and the primary determinant of bioactive LPA in the circulation. Mouse model studies have revealed an important role for the ATX-LPA receptor axis in tumor progression as well as in other pathologies, ranging from inflammation to fibrosis (2, 12–21). Accordingly, pharmacological inhibition of ATX is an attractive way to interfere with LPA signaling for therapeutic benefit. Most ATX inhibitors described so far are LPA analogs, whose designs are based on the initial observation that LPA can act as a feedback inhibitor in vitro and that LPA binds to ATX with much higher apparent affinity than the substrate LPC does (22). However, we found that synthetic LPA analogs and related lysophospholipids, such as the S1P analog FTY720-phosphate (26), are rather poor ATX inhibitors in the presence of high LPC concentrations.

In this study we have identified and optimized a class of thiazolidinedione compounds as potent and selective inhibitors of ATX. Our chemical optimization strategy was based on targeting the catalytic T210 residue in ATX by introducing a boronic acid moiety. Boronic acid has previously been shown to be instrumental in the anticancer drug bortezomib, which targets the threonine oxygen nucleophile in the active site of the proteasome (30). Strikingly, replacing the carboxylic acid in **HA51** by a boronic acid increased the potency for ATX inhibition by two orders of magnitude compared to the screening hit **A**. The boronic acid **HA130** has an IC_{50} value of 28 nM using LPC (40 μM) as a substrate and did not affect either NPP1 or proteasome activity. Injection of **HA130** into mice resulted in a rapid fall in circulating LPA levels, which is in keeping with the rapid degradation of intravenous administered C17-LPA observed in these animals. This result indicates that maintenance of steady-state LPA levels in plasma involves a highly dynamic balance between its ATX-mediated synthesis and its degradation by LPPs. Consistent with this, LPP1-deficient mice show a significantly reduced rate of [^{32}P]LPA degradation in the bloodstream (32). Thus, ATX and LPPs are key determinants of LPA turnover in vivo and their activity balance sets the steady-state level of LPA in the circulation and, most likely, in the interstitial space.

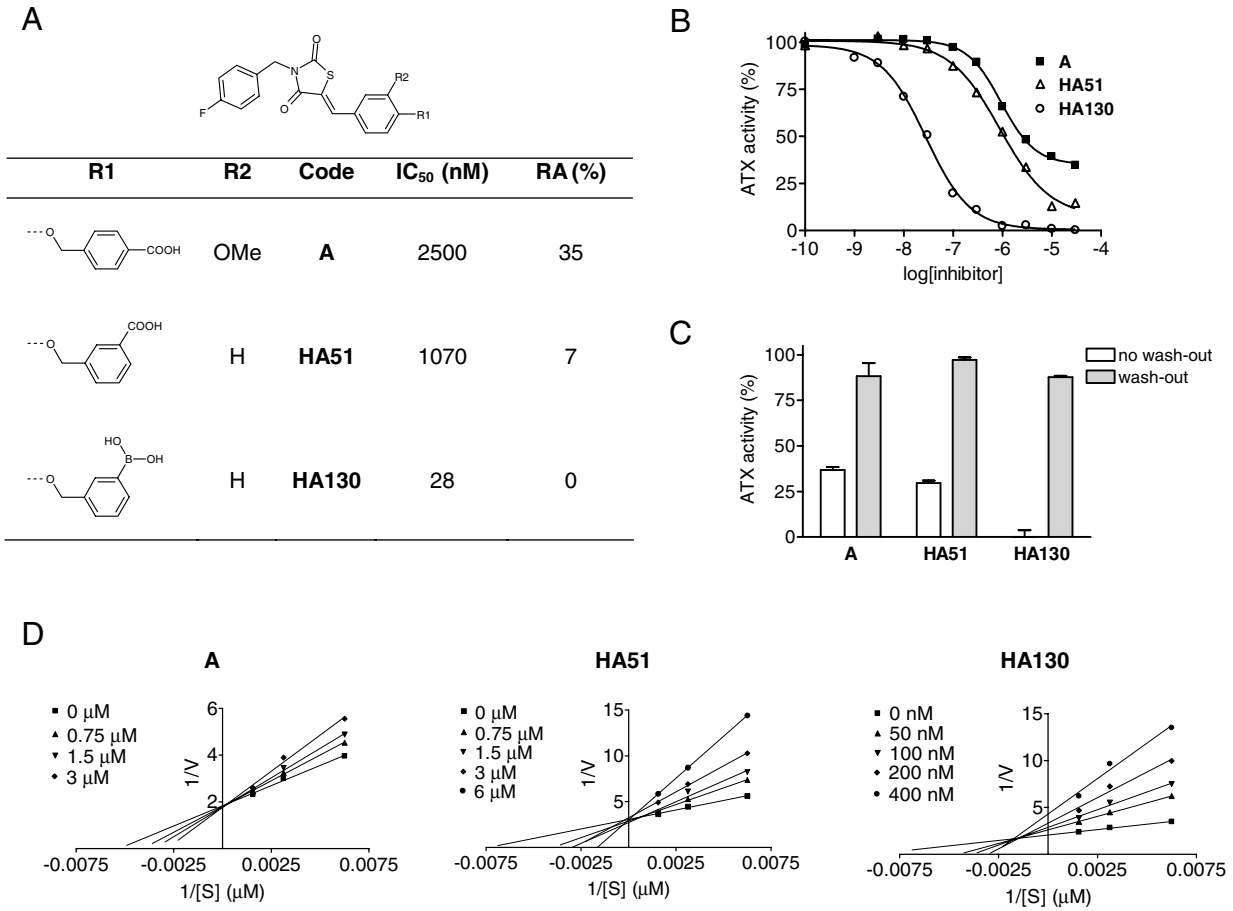

Fig. 3. Analysis of ATX inhibition by compounds **A**, **HA51**, and boronic acid-based **HA130**, as measured by choline release from LPC (40 μM). (*A*) IC_{50} values and residual ATX activity for the three inhibitors tested. (*B*) Dose-inhibition curves for the compounds shown in (*A*). (*C*) Wash-out experiments showing that ATX inhibition is reversible. (*D*) Lineweaver-Burk plot analysis of ATX inhibition, showing competitive inhibition by compounds **A** and **HA51**, and mixed-type inhibition by **HA130**. For details *SI Text*.

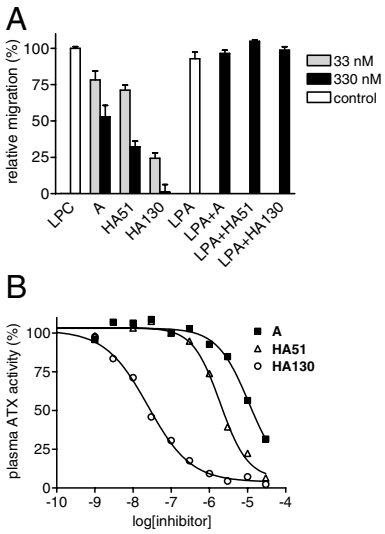

Fig. 4. Effect of inhibitors on ATX-induced cell migration and on plasma ATX/lysoPLD activity. (*A*) ATX (1.2 nM), LPC (1 μM), and BSA (1 mg mL^{-1}) were added to the lower chambers of 48-wells Boyden chambers and the transwell migration of A2058 melanoma cells was assayed after 4 h in the presence or absence of ATX inhibitors. None of the compounds inhibited LPA-induced cell migration (LPA added at 0.3 μM). (*B*) Inhibition of endogenous ATX/lysoPLD activity in human plasma ex vivo, as measured by choline release from LPC. Inhibition was maintained for at least 24 h (Table S1).

Several questions concerning circulating ATX remain to be answered, including its tissue origin and metabolic fate, although recent evidence indicates that ATX is rapidly cleared from the circulation by liver sinusoidal endothelial cells (33). Circulating ATX and LPA do not, of course, reflect the levels in intercellular spaces, since ATX is produced locally by many different cell types while the LPC substrate level in interstitial fluids is much lower than that in plasma. Another key question concerns how ATX activity is regulated under (patho)physiological conditions. Interestingly, ATX binds to activated lymphocytes and platelets in an integrin-dependent manner (18 and 21), which could lead to altered catalytic activity and serve as a mechanism for localized LPA production at sites of inflammation and injury.

In conclusion, we have used a boronic acid-based inhibitor to demonstrate that ATX is a valid target for manipulating LPA levels in vivo. Further development of boronic acid inhibitors of ATX holds promise for therapeutic use in ATX/LPA-dependent pathologies, including chronic inflammation, tumor progression, and fibrotic diseases.

Methods

ATX/lysoPLD Activity Assay. ATX/lysoPLD activity was measured by choline release from LPC (18:1) (80 μM) in 96-well plates. Inhibitors (5 μM) in DMSO were added to recombinant ATX (40 nM) in Tris-HCl buffer (pH 7.4) at 37 °C. After 3 h of incubation, 50 μL 2,2′-azino-bis(3-ethylbenzothiazoline-6-sulfonic acid) (ABTS) (2 mM) and horseradish peroxidase (10 Unit mL^{-1}) were added to 50 μL of the reaction mixture. Choline oxidase (50 μL, 10 Unit mL^{-1}) was added for the colorimetric reaction. Absorbance was measured at 405 nm and data were analyzed using Graphpad Prism software.

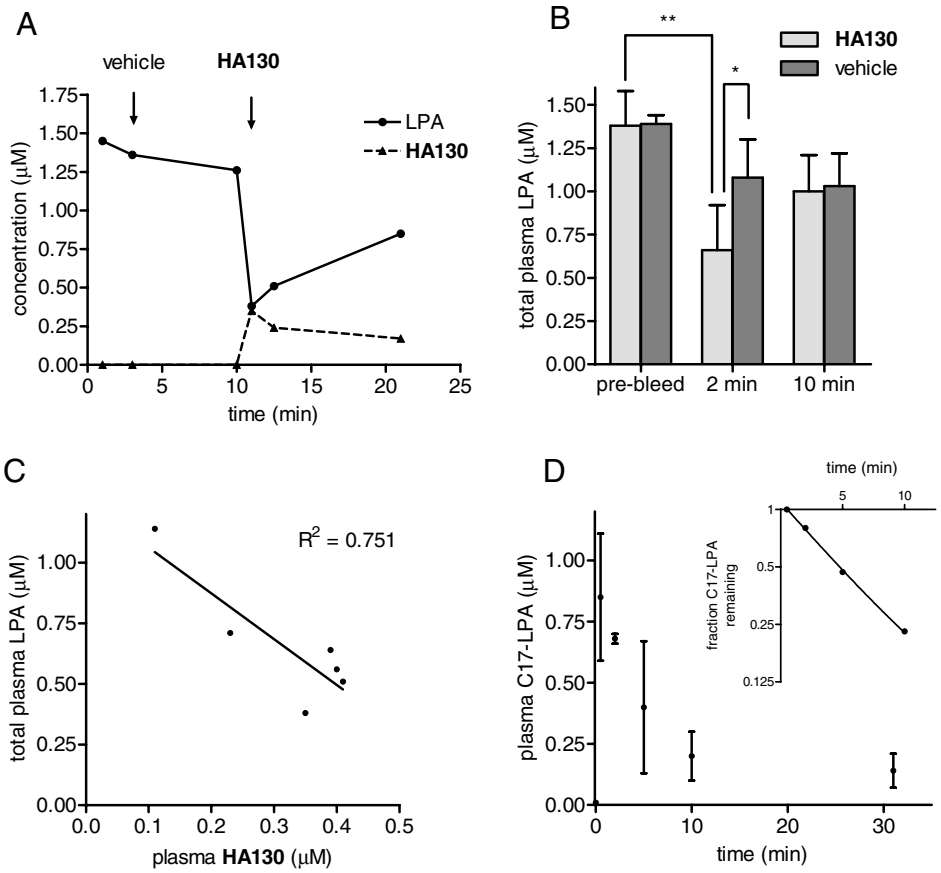

Fig. 5. Effects of **HA130** on circulating LPA levels in mice. (*A*) Vehicle or **HA130** was administered intravenously into an anaesthetized mouse and plasma levels of the inhibitor or total LPA were determined at the indicated time points. Compound **HA51** was used as a nonvehicle control (Fig. S5). (*B*) Plasma levels of LPA were determined at baseline and at 2 and 10 min post dosing of vehicle or **HA130**. The data shown are means + / − SD (six mice treated with **HA130**; five mice treated with vehicle alone). The difference between baseline LPA levels and LPA levels at 2 min in drug-treated mice are statistically significant ($P = 0.001$) by paired t-test. (*C*) Plasma levels of LPA and **HA130** at 2 min post administration closely correlate ($R^2 = 0.751$). (*D*) C17-LPA (10 μL of a 10 mM solution in saline containing 0.1% fatty acid-free BSA) was injected into the jugular vein of anaesthetized mice and plasma levels of C17-LPA were determined at different time points. The inset shows a semilog plot used to calculate the half-life for clearance of C17-LPA from the circulation. Data points are means + / − SD (n = 3).

Human Plasma ATX Activity. Plasma ATX activity was measured in 96-wells plates using LPC (18:1) as a substrate. Heparin-treated human plasma (2 μL) was added to 38 μL Tris-HCl buffer (100 mM Tris-HCl, pH 9, 500 mM NaCl, 5 mM $MgCl_2$ and 0.05% Triton X-100). Subsequently, 0.8 μL inhibitor in DMSO was added. Finally, 40 μL of 2 mM LPC (18:1) in Tris-HCl buffer was added to each well and the plate was incubated at 37 °C. The mixture with DMSO alone was used as a control. Plasma without added LPC was taken as control for endogenous LPA production. After 1.5 h of incubation, 150 μL homovanillic acid (2 mM) and horseradish peroxidase (1.6 Unit mL^{-1}) in Tris-HCl (0.01% Triton X-100, 20 mM $CaCl_2$ and 50 mM Tris-HCl, pH = 7.4) was added to 20 μL of the reaction mixture. Choline oxidase was added (40 μL, 4 Unit mL^{-1}) and fluorescence was determined at $\lambda_{ex}/\lambda_{em}$ = 320/450 nm.

ATX-Mediated Cell Migration. A2058 melanoma cell chemotaxis was assayed using 48-well Boyden chambers. Fibronectin-coated polycarbonate membranes (8 μM pores, NeuroProbe Inc.) were used to separate the upper from the lower chamber. The lower chamber contained DMEM with BSA (1 mg mL^{-1}), ATX (1.2 nM) and LPC (1 μM). Cells (0.75×10^6 mL^{-1}) were loaded in the upper wells and the chamber was incubated at 37 °C for 4 h. Nonmigrated cells were removed from the membrane and migrated cells were fixed and stained in Diff-Quick (Medion Diagnostics AG). The membrane was mounted on a glass slide and migrated cells were quantified.

Studies in Mice. For intravenous administration, **HA130** and **HA51** in DMSO were diluted 10-fold into saline to give a drug concentration solution of 1 mM and a final DMSO concentration of 10%. This material was kept at 37 °C and bath sonicated for 30 s immediately prior to intravenous administration. Male FVB mice were anaesthetized with isofluorane and dissected to expose the jugular vein. **HA130** (1 μL g^{-1}, 1 mM) or vehicle were injected intravenously. **HA51** served as a nonvehicle control. Whole blood was sampled from the jugular vein and collected directly into anticoagulant, mixed, centrifuged, and plasma transferred to glass tubes containing acidified solvents for extraction of **HA130** and LPA. All animal experiments conformed to the recommendations of the "Guide for the Care and Use of Laboratory Animals" (Department of Health, Education, and Welfare publication number NIH 78-23, 1996) and were approved by the institutional Animal Care and Use Committee.

Additional assays and chemical synthesis: *SI Text*.

ACKNOWLEDGMENTS. We thank Anastassis Perrakis and Andreas Kremer for helpful discussions. This work was supported by grants from the Netherlands Organization for Scientific Research (NWO) (to H.O., W.H.M.), the Dutch Cancer Society (to W.H.M.), the Center for Biomedical Genetics (to W.H.M.), the Netherlands Genomics Initiative (to H.O.), and the National Institutes of Health (NIH; HL074219 and HL078663 (to S.S.S.)); and GM050388 (to A.J.M.).

1. Stracke ML, et al. (1992) Identification, purification, and partial sequence analysis of autotaxin, a novel motility-stimulating protein. *J Biol Chem* 267:2524–2529.
2. van Meeteren LA, Moolenaar WH (2007) Regulation and biological activities of the autotaxin-LPA axis. *Prog Lipid Res* 46:145–160.
3. Umezu-Goto M, et al. (2002) Autotaxin has lysophospholipase D activity leading to tumor cell growth and motility by lysophosphatidic acid production. *J Cell Biol* 158:227–233.
4. Tokumura A, et al. (2002) Identification of human plasma lysophospholipase D, a lysophosphatidic acid-producing enzyme, as autotaxin, a multifunctional phosphodiesterase. *J Biol Chem* 277:39436–39442.
5. Stefan C, Jansen S, Bollen M (2005) NPP-type ectophosphodiesterases: unity in diversity. *Trends Biochem Sci* 30:542–550.
6. Noguchi K, Herr D, Mutoh T, Chun J (2009) Lysophosphatidic acid (LPA) and its receptors. *Curr Opin Pharmacol* 9:15–23.

7. Moolenaar WH, van Meeteren LA, Giepmans BN (2004) The ins and outs of lysophosphatidic acid signaling. *Bioessays* 26:870–881.
8. Sciorra VA, Morris AJ (2002) Roles for lipid phosphate phosphatases in regulation of cellular signaling. *Biochim Biophys Acta* 1582:45–51.
9. Brindley D, Pilquil C (2009) Lipid phosphate phosphatases and signaling. *J Lipid Res* 50:S225–S230.
10. Tanaka M, et al. (2006) Autotaxin stabilizes blood vessels and is required for embryonic vasculature by producing lysophosphatidic acid. *J Biol Chem* 281:25822–25830.
11. van Meeteren LA, et al. (2006) Autotaxin, a secreted lysophospholipase D, is essential for blood vessel formation during development. *Mol Cell Biol* 26:5015–5022.
12. Mills GB, Moolenaar WH (2003) The emerging role of LPA in cancer. *Nat Rev Cancer* 3:582–591.
13. Taghavi P, et al. (2008) In vitro genetic screen identifies a cooperative role for LPA signaling and c-Myc in cell transformation. *Oncogene* 27:6806–6816.
14. Nam SW, et al. (2000) Autotaxin (ATX), a potent tumor motogen, augments invasive and metastatic potential of ras-transformed cells. *Oncogene* 19:241–247.
15. Liu S, et al. (2009) Expression of autotaxin and lysophosphatidic acid receptors increases mammary tumorigenesis, invasion, and metastases. *Cancer Cell* 15:539–550.
16. Boucharaba A, et al. (2004) Platelet-derived lysophosphatidic acid supports the progression of osteolytic bone metastases in breast cancer. *J Clin Invest* 114:1714–1725.
17. Lin S, et al. (2009) The absence of LPA2 attenuates tumor formation in an experimental model of colitis-associated cancer. *Gastroenterology* 136:1711–1720.
18. Kanda H, et al. (2008) Autotaxin, an ectoenzyme that produces lysophosphatidic acid, promotes the entry of lymphocytes into secondary lymphoid organs. *Nat Immunol* 9:415–423.
19. Pradere JP, et al. (2007) LPA1 receptor activation promotes renal interstitial fibrosis. *J Am Soc Nephrol* 18:3110–3118.
20. Tager A, et al. (2008) The lysophosphatidic acid receptor LPA1 links pulmonary fibrosis to lung injury by mediating fibroblast recruitment and vascular leak. *Nat Med* 14:45–54.
21. Pamuklar Z, et al. (2009) Autotaxin/lysopholipase D and lysophosphatidic acid regulate murine hemostasis and thrombosis. *J Biol Chem* 284:7385–7394.
22. van Meeteren LA, et al. (2005) Inhibition of autotaxin by lysophosphatidic acid and sphingosine 1-phosphate. *J Biol Chem* 280:21155–21161.
23. Baker DL, et al. (2006) Carba analogs of cyclic phosphatidic acid are selective inhibitors of autotaxin and cancer cell invasion and metastasis. *J Biol Chem* 281:22786–22793.
24. Cui P, et al. (2008) [alpha]- and [beta]-Substituted phosphonate analogs of LPA as autotaxin inhibitors. *Bioorg Med Chem* 16:2212–2225.
25. Ferry G, et al. (2008) S32826, A nanomolar inhibitor of autotaxin: Discovery, synthesis and applications as a pharmacological tool. *J Pharmacol Exp Ther* 327:809–819.
26. van Meeteren LA, et al. (2008) Anticancer activity of FTY720: phosphorylated FTY720 inhibits autotaxin, a metastasis-enhancing and angiogenic lysophospholipase D. *Cancer Lett* 266:203–208.
27. Parrill A, et al. (2008) Virtual screening approaches for the identification of non-lipid autotaxin inhibitors. *Bioorg Med Chem* 16:1784–1795.
28. Adams J, et al. (1998) Potent and selective inhibitors of the proteasome: dipeptidyl boronic acids. *Bioorg Med Chem Lett* 8:333–338.
29. Kropff M, et al. (2007) Bortezomib in combination with intermediate-dose dexamethasone and continuous low-dose oral cyclophosphamide for relapsed multiple myeloma. *Br J Haematol* 138:330–337.
30. Groll M, Berkers CR, Ploegh HL, Ovaa H (2006) Crystal structure of the boronic acid-based proteasome inhibitor bortezomib in complex with the yeast 20S proteasome. *Structure* 14:451–456.
31. Nakasaki T, et al. (2008) Involvement of the lysophosphatidic acid-generating enzyme autotaxin in lymphocyte-endothelial cell interactions. *Am J Pathol* 173:1566–1576.
32. Tomsig JL, et al. (2009) Lipid phosphate phosphohydrolase type 1 (LPP1) degrades extracellular lysophosphatidic acid in vivo. *Biochem J* 419:611–618.
33. Jansen S, et al. (2009) Rapid clearance of the circulating metastatic factor autotaxin by the scavenger receptors of liver sinusoidal endothelial cells. *Cancer Lett* 284:216–221.